SiC MOSFETs for Future Motor Drive Applications

S. Tiwari, O.-M. Midtgård, T. M. Undeland

Norwegian University of Science and Technology
7491 Trondheim, Norway
subhadra.tiwari@ntnu.no

Keywords

≪Silicon Carbide (SiC)≫, ≪MOSFET≫, ≪IGBT≫, ≪Conduction losses≫, ≪Switching losses≫, ≪Efficiency≫, ≪Simulation≫.

Abstract

This paper investigates the switching performance of six-pack SiC MOSFET and Si IGBT modules for motor drive applications. Both the modules have same packaging and voltage rating (1.2 kV). The three bridge legs of the modules are paralleled forming a single half-bridge configuration for achieving higher output power. Turn-on and turn-off switching energy losses are measured using a standard double pulse methodology. The conduction losses from the datasheet and the switching energy losses obtained from the laboratory measurements are used as a look up table input when simulating the detailed inverter losses in a three-phase motor drive inverter. The total inverter loss is plotted for different switching frequencies in order to illustrate the performance improvement that SiC MOSFETs can bring over Si IGBTs for a motor drive inverter from the efficiency point of view. The overall analysis gives an insight into how SiC MOSFET outperforms Si IGBT over all switching frequency ranges with the advantages becoming more pronounced at higher frequencies and temperatures.

Introduction

Medium voltage motor drives will benefit from the superior material properties of SiC. For instance, SiC devices offer a breakdown electric field of ten times higher than Si devices. This allows more heavily doped and shorter drift layer structures, resulting in very low specific on-state resistance even at high blocking voltages, thus reducing the conduction loss with a promise for higher power rating [1]. Therefore, when SiC MOSFETs become available in the 10 kV range, they can replace series connected Si IGBTs, and thereby the weight, volume and loss of the converter will be reduced.

In addition, the SiC devices offer three times higher bandgap and thermal conductivity compared to the Si devices. This means that the converter can be operated at a higher junction temperature [2, 3] and has a better heat dissipation, which eventually leads to less need for thermal management and cooling, also resulting in more compact converters. Motor drive inverters will also benefit from the fast switching feature of SiC devices provided a small dv/dt or sine wave filter is used between the inverter and the motor.

Moreover, the on-state resistance of a semiconductor power device is inversely proportional to the chip area. When the SiC becomes cheaper, the chip area can be made bigger in high performance drives so that the on-state resistance is reduced, thereby further reducing the conduction loss.

By adjusting the doping concentration, SiC MOSFETs can be produced according to application requirements. For example, for fast switching applications, higher speed can be prioritized whereas for slow switching applications, on-state voltage can be the main criterion. Considering the motor drive application, manufacturers have started to look into different structures that give reduced on-state losses; for instance, a double trench structure has been discussed in [4].

Several papers have been published regarding the use of the SiC devices for motor drive applications. For example: benefits of using a SiC diode instead of a Si PiN diode as a free-wheeling diode in a IGBT for a three-phase motor drive converter is discussed in [5]. The switching performance of discrete SiC MOSFET is evaluated in a PWM inverter fed induction motor drives in [6, 7]. The use of six-pack SiC MOSFET module is compared with Si IGBT module at different switching frequencies in [8].

However, this paper focuses on comparing the total loss for SiC MOSFETs (CCS050M12CM2, 50 A) and Si IGBTs (FS75R12KT4_B15, 75A) in a three-phase motor drive inverter formed by paralleling of the three-bridge legs inside one module, using one module for each phase. In order to carry out a fair comparison between the two technologies, both of the SiC MOSFET and Si IGBT modules are chosen with similar voltage rating and packaging. Fig. 1 a) shows the package of the SiC module used in the measurements. Even though the current rating of SiC MOSFET module is 50 A and Si IGBT is 75 A, the comparison of loss is made at the same current value (50 A).

The converter losses are compared for two different cases. In the first case, the gate resistance (R_g) is optimized for the Si IGBT as a trade-off among switching losses, acceptable dv/dt, and overshoots. The detailed switching performances are illustrated for both modules maintaining approximately the same dv/dt by slowing down the SiC MOSFET. The turn-on and turn-off behaviours are also studied at various temperatures and load currents.

In the second case, the R_g for the SiC MOSFET is optimized with a trade-off between both current and voltage overshoot and switching loss. The R_g for the Si IGBT is kept equal to that of the SiC MOSFET. The detailed switching performances and losses are illustrated in a previous work [9]. In this paper, the measured conduction and switching energy losses are used as a look up table input in a MATLAB Simulink simulation of a three-phase motor inverter circuit to observe the losses.

Methodology and measurement setup

For measuring the turn-on and turn-off switching energy losses, a standard double pulse methodology is used, which allows to do the measurements with known junction temperature (T_j) [10]. In order to have a comparable stray inductance as in a real application circuit, a three-phase inverter power circuit board, acting as a strip line connection between the module and the dc-link capacitors, was built, and a six-pack module is mounted such that the three bridge legs are paralleled forming a single half-bridge, as shown in Fig. 1 b). A negative voltage of 5 V is applied for the upper MOSFETs in order to ensure that they are turned off all the time. For the lower MOSFETs, a gate voltage of 20 V is applied during turn-on and -5 V during turn-off. For each measured current, the first turn-off and the second turn-on waveforms are recorded. A single layer inductive load is used in order to ensure the minimum stray capacitance [11]. The complete laboratory hardware setup is depicted in Fig. 2. The Si IGBT is driven by the same gate driver as that for the SiC MOSFET, except a small modification for obtaining $\pm$15 V required for driving an IGBT.

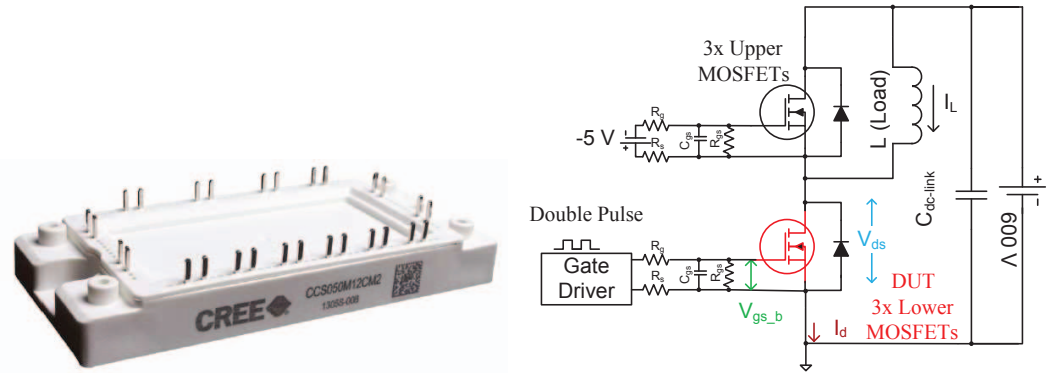

(a) Photo of six-pack MOSFET module.

(b) Circuit diagram.

Fig. 1: Photo of SiC MOSFET module from Cree and circuit diagram. The upper and the lower three transistors are paralleled, forming a single half-bridge configuration.

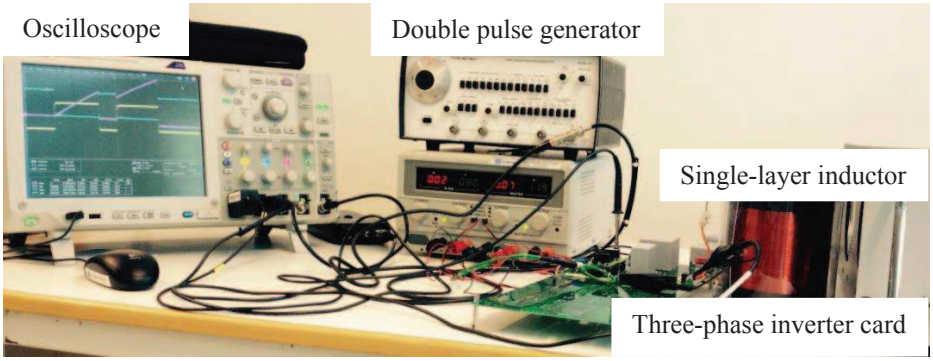

Fig. 2: Hardware setup showing the double pulse test arrangement. Switching energy loss is measured using a three-phase inverter power circuit board in order to emulate a stray inductance of a real application circuit.

Table I shows the key electrical parameters of the SiC MOSFET versus the Si IGBT taken from the manufacturers datasheet [15, 16]. R_{ds} / R_{ce} is the on-state resistance of MOSFET / IGBT, V_{CEO} is the on-state zero-current collector-emitter voltage, and R_d is the resistance of the free-wheeling diode. The SiC MOSFET shows higher temperature dependency compared to the Si IGBT.

Table I: Key electrical parameters of SiC MOSFETs module versus Si IGBT module.

	CCS050M12CM2 (Cree)			FS75R12KT4_B15 (Infineon)		
Parameters	25 (°C)	125 (°C)	difference (%)	25 (°C)	125 (°C)	difference (%)
R_{ds} / R_{ce} $(m\Omega)$	25	39.4	+57.6	11.1	15.51	+39.7
V_{CEO} (V)	Absent	Absent	Absent	1	0.84	−16
R_d $(m\Omega)$, diode	10	19.77	+97.7	9.46	10.62	+12.2
V_{FO} (V), diode	0.85	0.77	−9.4	1.05	0.93	−11.4

Laboratory testing of SiC MOSFET versus Si IGBT module

Switching transients with varying gate resistance

The value of R_g for the SiC MOSFET module is selected such that the dv/dt is similar to the results for the Si IGBT module at a junction temperature of 25 °C. As shown in Fig. 3 a), c) and e), both the current and voltage overshoots are reduced with increased R_g because the switching becomes slower.

For generation 4 trench field stop IGBT, the turn-off process is decided by the intrinsic behaviour of the device for the lower gate resistances. However, if R_g is increased above a certain range, the dv/dt decreases but the voltage overshoot increases, which is due to the stored charge in the device during turn-on [13]. This phenomenon is elucidated in Fig. 3 d). Therefore, R_g of 2.2 Ω is selected as the trade-off among switching losses, acceptable dv/dt and overshoot as per the requirement of the application.

Table II shows a sample of switching energy loss for the SiC MOSFET versus the Si IGBT with a dc-link voltage of 500 V and a load current of 120 A at a junction temperature of 25 °C, for two different values of R_g, for each module. dv/dt is the voltage slew rate during turn-off and di/dt is the current slew rate during turn-on of the device under test. The turn-off loss (E_{off}) in the Si IGBT is relatively high and is almost similar at both high (20 Ω) and low (12.2 Ω) R_g. This is primarily governed by the intrinsic phenomenon within the IGBT structure. In particular, the recombination process and the charge carrier lifetime being independent of R_g. On the other hand, the turn-off loss of the SiC MOSFET decreases remarkably with decrease in R_g, which is mainly because of the unipolar nature of the device. The turn-on loss (E_{on}) of both devices depends strongly on R_g. The reverse recovery loss of the diode (E_{rec}) in both the Si and SiC diodes decreases slightly with increasing R_g.

Table II: Key measurements of SiC MOSFET vs Si IGBT module. V_{ds} = 500 V and I_{ds} = 120 A.

Device Under Test (DUT)	R_g (Ω)	dv/dt (V/ns)	di/dt (A/ns)	E_{off} (mJ)	E_{on} (mJ)	E_{rec} (mJ)
CCS050M12CM2 (Cree)	36.5	4.25	1.33	3.86	6.95	0.11
	20	8.49	2.63	1.28	3.26	0.22
FS75R12KT4_B15 (Infineon)	12.2	4.37	2.28	6	8.43	2.46
	20	4.42	1.43	6.36	14.13	2.34

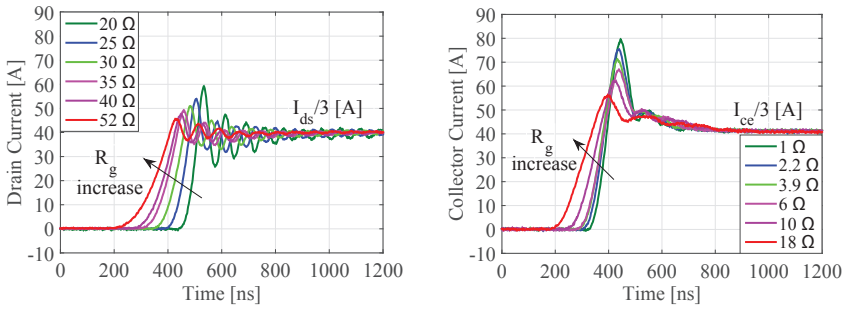

(a) Turn-on transient of the MOSFET.

(b) Turn-on transient of the IGBT.

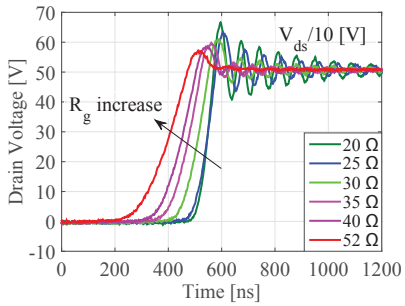

(c) Turn-off transient of the MOSFET.

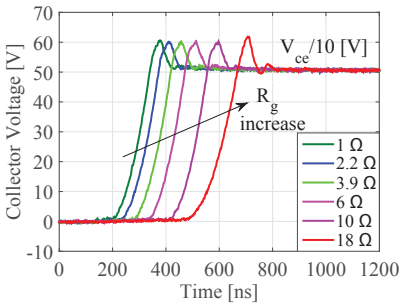

(d) Turn-off transient of the IGBT.

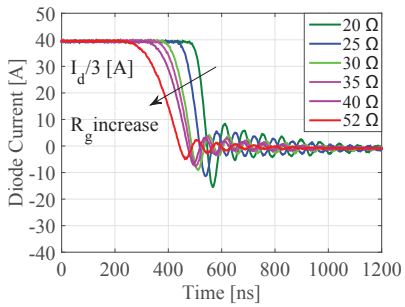

(e) Turn-off transient of the SiC SBD.

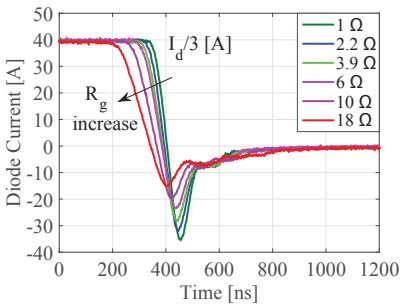

(f) Turn-off transient of the Si diode.

Fig. 3: Drain/collector current, drain/collector voltage and diode current with varying R_g for the SiC MOSFET versus the Si IGBT module. The chosen equivalent R_g per chip for the SiC MOSFET is 36.5 Ω with an external R_g of 35 Ω and internal 1.5 Ω. For the Si IGBT module, the chosen equivalent R_g per chip is 12.2 Ω with an external R_g of 2.2 Ω and internal 10 Ω. This combination of R_g results in similar dv/dt in each module during turn-off.

Switching transients with varying load current

In this subsection, the dc-link voltage is set to 500 V while the load current is increased from 30 A to 150 A. It can be observed from Fig. 4 that the di/dt of the current in the SiC MOSFET and the diode increases slightly, while the dv/dt of the MOSFET voltage increases noticeably. This part of behaviour

in the SiC MOSFET also corresponds to that of the Si IGBT. However, the peak reverse current of the SiC anti-parallel diode remains almost constant at all the load current which is depicted in Fig. 4 e). Conversely, the peak reverse recovery current of the Si anti-parallel diode increases with the increase of the load current, which is apparent from Fig. 4 f).

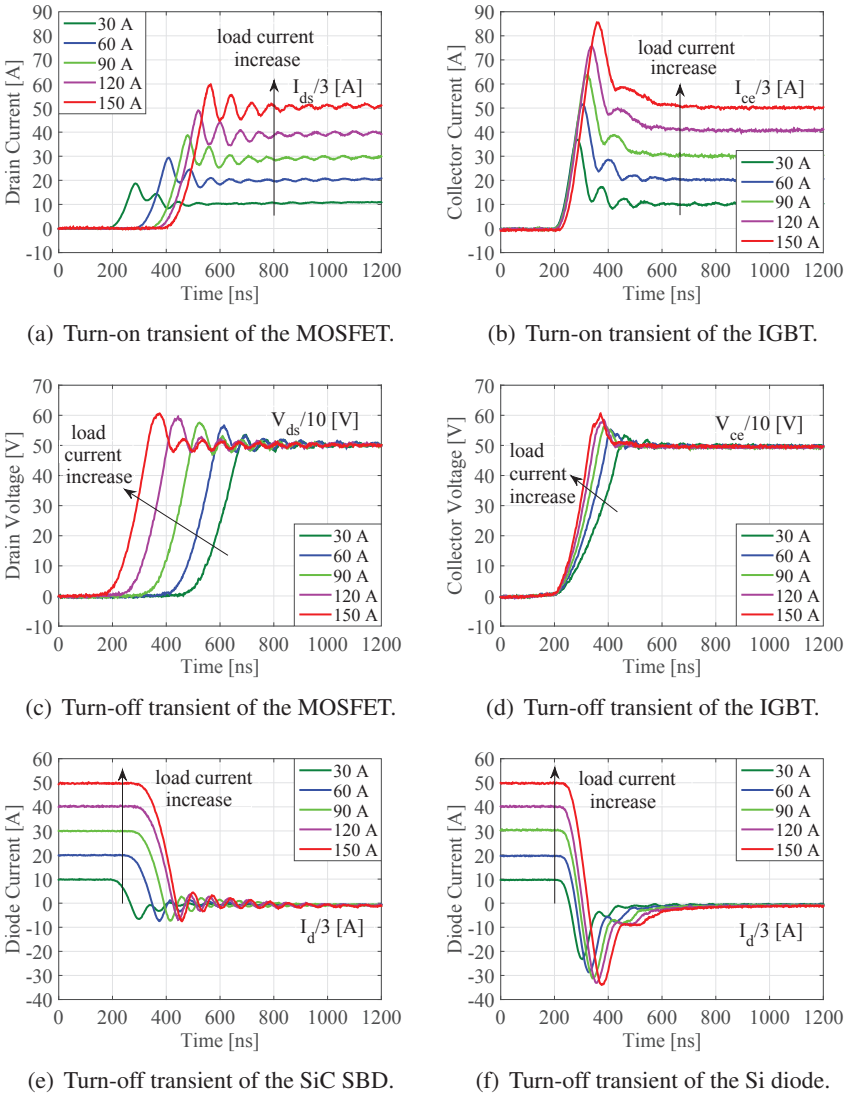

(a) Turn-on transient of the MOSFET.

(b) Turn-on transient of the IGBT.

(c) Turn-off transient of the MOSFET.

(d) Turn-off transient of the IGBT.

(e) Turn-off transient of the SiC SBD.

(f) Turn-off transient of the Si diode.

Fig. 4: Drain/collector current, drain/collector voltage and diode current with varying load current for the SiC MOSFET versus the Si IGBT. For the SiC MOSFET, R_g is 36.5 Ω and for the Si IGBT, it is 12.2 Ω.

Switching transients with varying junction temperature

In this subsection, the dc-link voltage is set to 500 V and the load current to 120 A while the junction temperature is increased from 25 °C to 125 °C. With the increased temperature, the turn-on of SiC MOSFET becomes slightly faster because of the negative temperature coefficient of gate threshold voltage, and therefore leads to a decrease in the turn-on switching energy loss. The SiC MOSFET module is copacked with SiC Schottky barrier diode (SBD) as an anti-parallel diode. The reverse-recovery charge in the SiC SBD is extremely low compared to Si diode [9]. This charge is not due to conductivity modulation as in Si diode and is independent of temperature, forward current and di/dt as inferred from these characterization and also conforms with [12].

In the Si IGBT module, the Si diode is present as a free-wheeling diode. It is evident from Fig. 5 b) and f) that the reverse recovery current present at turn-off of the diode directly affects the current peak during the turn-on of the Si IGBT. This peak worsens with increased operating temperature. During the

turn-off, the voltage overshoot decreases a little as the turn-off voltage rise slows down with increased temperature, as seen in Fig. 5 d).

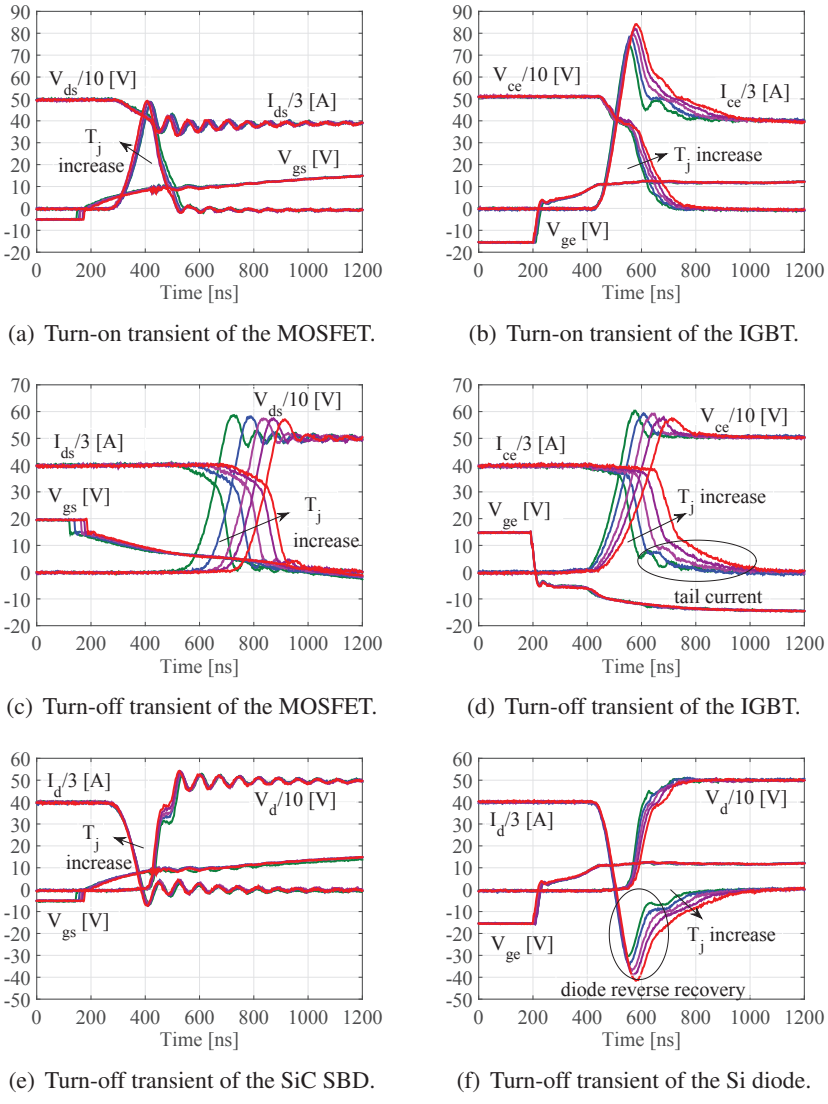

(a) Turn-on transient of the MOSFET.

(b) Turn-on transient of the IGBT.

(c) Turn-off transient of the MOSFET.

(d) Turn-off transient of the IGBT.

(e) Turn-off transient of the SiC SBD.

(f) Turn-off transient of the Si diode.

Fig. 5: Drain/collector current, drain/collector voltage and diode current with varying junction temperature for the SiC MOSFET versus the Si IGBT module. For the SiC MOSFET, R_g is 36.5 Ω and for the Si IGBT, it is 12.2 Ω.

Table III shows a sample of key measurements taken for the two modules at 125 °C. With the increase in temperature, E_{rec} increases substantially in the Si diode, whereas it is slightly increased or almost unaffected by the temperature in the SiC SBD. Furthermore, it should be noted that the E_{rec} increases with the decrease in R_g, unlike in the SiC MOSFET or the Si IGBT where the switching loss decreases with the decrease in R_g.

Simulation of the converter losses

The three-phase inverter fed induction motor drive as shown in Fig. 6 is simulated in MATLAB. The switching loss obtained from the laboratory measurements and the conduction loss from the datasheet are used as a lookup table input for calculating the total converter loss. The loss is calculated for an open loop space vector PWM, with a power factor of 0.85, a modulation index of 1, a dc-link voltage of 760 V, and a load current of 150 A. The converter output voltage is about 460 V and the power rating is approximately 100 kW.

Table III: Key measurements of SiC MOSFET vs Si IGBT module. V_{ds} = 500 V and I_{ds} = 120 A.

Device Under Test (DUT)	R_g (Ω)	dv/dt (V/ns)	di/dt (A/ns)	E_{off} (mJ)	E_{on} (mJ)	E_{rec} (mJ)
CCS050M12CM2 (Cree)	36.5	4.08	1.5	4.08	6.28	0.12
	20	8	2.89	1.54	2.57	0.35
FS75R12KT4_B15 (Infineon)	12.2	2.7	2.41	10.67	12.9	9.37
	20	2.4	1.5	10.36	18.36	7.7

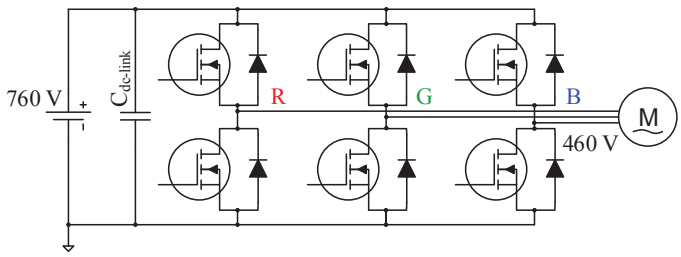

Fig. 6: Schematic diagram of a three-phase motor drive inverter with induction motor as a load.

Evaluation of inverter power loss at varying switching frequency

The detailed loss breakdown at two different temperatures (25 °C and 125 °C), and various switching frequencies (1 kHz to 100 kHz) are shown in Fig. 7 a) and b). Simulation results show that the conduction loss in the Si IGBT inverter is a factor of 1.14 at 25 °C and a factor of 0.77 at 125 °C to that in the SiC MOSFET inverter. For the low frequency region, the conduction loss is a dominating part of total inverter loss for both the MOSFET and IGBT, which is also apparent from bar chart in Fig. 7.

Furthermore, Fig. 7 a) which is a case with 25 °C, reveals that conduction loss and switching loss are approximately equal for the Si at 10 kHz and for the SiC at 25 kHz. Likewise, it is clear from Fig. 7 b), which is the case with 125 °C, that these losses are almost equal at 4 kHz for the Si and at 35 kHz for the SiC. However, the total loss is comparable for both the SiC MOSFET and Si IGBT only upto 3 kHz, with the MOSFET showing slightly better performance than the IGBT.

Table IV shows that the inverter using the SiC MOSFET has significantly lower total switching energy loss (denoted by P_{sw} in Table IV, which is the sum of switching power loss of the transistors and diodes in a three-phase inverter) compared to the one using the Si IGBT. Depending on R_g, the ratio of switching loss in the Si to that in the SiC can be a factor of 1.55 to 4.79 at 25 °C and a factor of 3.5 to 8.6 at 125 °C.

Table IV: The ratio of switching loss in the Si to that in the SiC at 5 kHz, shown in the column "factor".

Temperature	25 °C			125 °C		
Conditions	P_{sw} W, SiC	P_{sw} W, Si	Factor	P_{sw} W, SiC	P_{sw} W, Si	Factor
Same dv/dt	280	433	1.55	270	941	3.5
Same R_g	122	585	4.79	118	1013	8.6
Optimized R_g	122	433	3.54	118	941	7.97

Table V: For the same output power and losses, a factor by which switching frequency in SiC can be increased to that in Si is given in the column "f_1/f_2".

Temperature	25 °C			125 °C		
Conditions	P_{tot} kW, SiC, f_1	P_{tot} kW, Si, f_2	f_1/f_2	P_{tot} kW, SiC, f_1	P_{tot} kW, Si f_2	f_1/f_2
Same dv/dt	6.17 (100 kHz)	6.2 (64 kHz)	1.56	6.28 (100 kHz)	6.32 (30 kHz)	3.3
Same R_g	3.01 (100 kHz)	3.0 (20 kHz)	5	3.23 (100 kHz)	3.11 (12 kHz)	8.3
Optimized R_g	3.01 (100 kHz)	2.99 (27 kHz)	3.7	3.23 (100 kHz)	3.12 (13 kHz)	7.7

Depending on R_g, for the same current (output power), inverter switching frequency can be increased by 1.56 to 5 times at 25 °C and 3.3 to 8.3 times at 125 °C in the SiC MOSFET compared to the Si IGBT with almost the same total power loss (P_{tot}) as presented in Table V.

For the converter with the Si IGBT, the combined loss of P_{sw-on} (turn-on loss) and P_{rec} (recovery loss) comprises the major portion of the total converter loss, specially at higher switching frequencies. In the case of optimized R_g (displayed in Fig. 7), this loss is 59.95 % of the total inverter loss at 25 °C, and 68.44 % at 125 °C for the Si at 100 kHz. Thus, it can be deduced that the Si IGBT is not a viable solution at high switching frequency. Therefore, a practical solution for reducing the total loss would be the use of SiC diode as an anti-parallel diode in the Si IGBT.

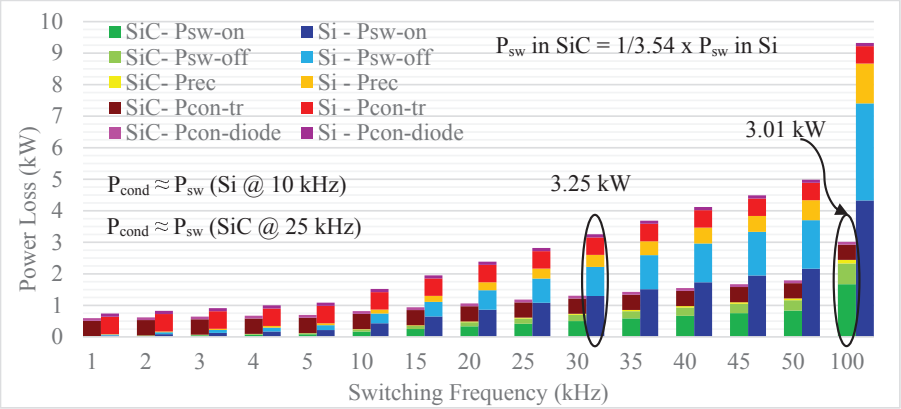

(a) Power Loss versus frequency at 25 °C. Frequency can be 3.3 times in SiC compared to Si.

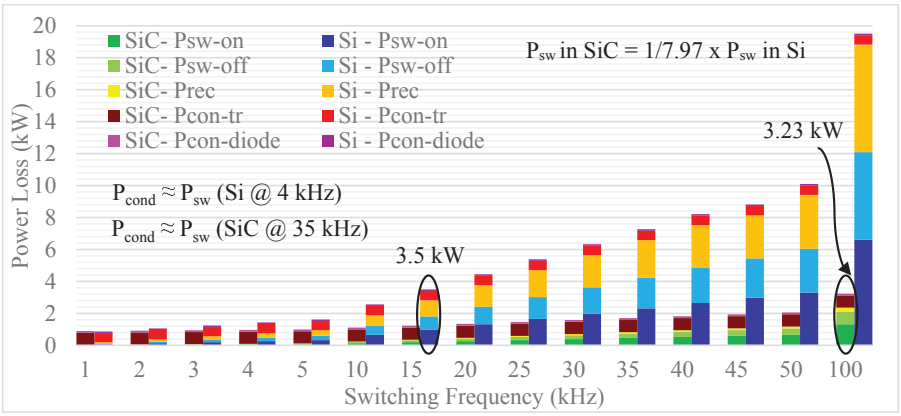

(b) Power Loss versus frequency at 125 °C. Frequency can be 6.6 times in SiC compared to Si.

Fig. 7: Breakdown of power loss in a converter at varying switching frequency for two different junction temperatures (25 °C and 125 °C) for the case with optimized R_g. The legends in bar chart are: turn-on switching loss (P_{sw-on}), turn-off switching loss (P_{sw-off}), diode recovery loss (P_{rec}), conduction loss in a transistor ($P_{cond-tr}$), and conduction loss in a diode ($P_{cond-diode}$). The converter losses are comparable at low switching frequencies ($\leq$ 3 kHz) for both modules. SiC MOSFET helps to reduce the switching loss, which is a dominant part of total loss in an IGBT inverter particularly at high switching frequencies.

Evaluation of inverter efficiency at varying switching frequency

A comparison of the total inverter efficiency using the all-SiC devices with the all-Si devices are shown in Fig. 8. The simulations are carried out at a junction temperature of 25 °C and 125 °C at two different R_g for each module. The efficiency (denoted as E_{ff} in Table VI) of the inverter using the SiC devices is almost independent of the operating temperature, while the power loss of the inverter using the Si devices shows strong temperature dependence, decreasing the efficiency from 91.68 % to 84.04 % (for R_g = 12.2 Ω) at 100 kHz, which is also indicated in Fig. 8. This is due to the strong temperature

dependence of the reverse recovery current of the Si free-wheeling diode and the tail current of the IGBT as discussed in the earlier section. Table VI shows an example summary of the simulation results.

Table VI: Difference in efficiency caused by difference in temperature at two different R_g.

Conditions	Efficiency (%) @ frequency	CCS050M12CM2 (Cree)			FS75R12KT4_B15 (Infineon)		
		25 (°C)	125 (°C)	diff. (%)	25 (°C)	125 (°C)	diff. (%)
R_g=36.5 Ω (SiC)	E_{ff} (20 kHz)	98.37	98.13	0.24	97.73	95.85	1.88
R_g=12.2 Ω (Si)	E_{ff} (100 kHz)	94.33	94.24	0.09	91.68	84.04	7.64
R_g=20 Ω (SiC)	E_{ff} (20 kHz)	98.97	98.7	0.27	97.16	95.59	1.57
R_g=20 Ω (Si)	E_{ff} (100 kHz)	97.15	96.94	0.21	89.25	83.06	6.19

At switching frequency of 20 kHz, which is typically the highest operating frequency of today's IGBTs available for high frequency applications (particularly for hard switched applications), converter with the SiC MOSFET shows 1.24 % higher efficiency at 25 °C and 2.85 % at 125 °C over their Si IGBT counterparts, for the case with optimized R_g (i.e., R_g=20 Ω for SiC and R_g=12.2 Ω for Si) in each modules.

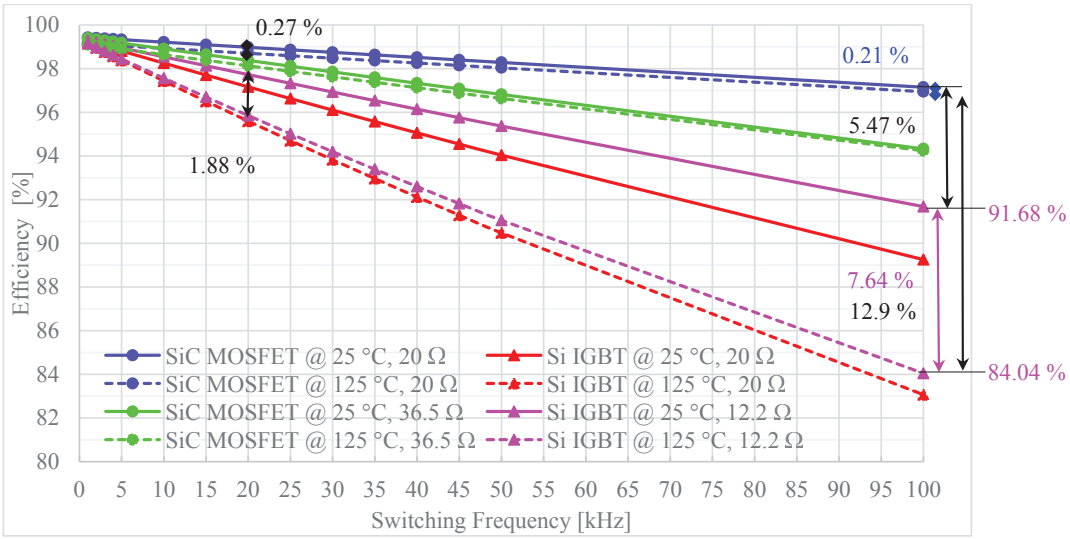

Fig. 8: Comparison of a 1.2 kV SiC MOSFET and 1.2 kV Si IGBT efficiencies in a three-phase inverter shows that at all the switching frequencies and temperatures, the higher efficiency SiC MOSFET provide a performance advantage over their Si IGBT counterparts. The efficiency of the converter using the SiC devices is almost independent of the operating temperature (a difference in efficiency of about 0.3 %) unlike the Si devices which show strong temperature dependence (a difference of 1.88 % at 20 kHz and 7.64 % at 100 kHz).

Fig. 8 further explains that the Si IGBT is not a practical solution at higher operating temperature, particularly when it is higher frequency as well. For example, at a switching frequency of 100 kHz and a junction temperature of 25 °C, the difference in efficiencies between the SiC and the Si is 5.47 %, while this difference is 12.9 % at 125 °C.

Conclusion

In this paper, a comparative study of two-level, three-phase inverter with a 1.2 kV SiC MOSFET and a 1.2 kV Si IGBT is carried out by simulation in MATLAB, in order to evaluate losses and efficiencies at different switching frequencies. The main conclusions derived from the paper are:

i) At lower switching frequencies, the conduction loss is the major contributor to the total converter loss. Even at the lowest switching frequency, the SiC MOSFET shows better performance than the Si IGBT.

ii) As the switching frequency increases, the share of switching power loss to the total converter loss increases, thereby the advantages of using the SiC MOSFET become more visible as it has lower switching loss compared to the Si IGBT. Depending on R_g, the ratio of switching loss in the inverter with the Si to that in the SiC can be a factor of 1.55 to 4.79 at 25 °C and a factor of 3.5 to 8.6 at 125 °C. Thus, for the same output power the inverter switching frequency can be increased by 1.56 to 5 times at 25 °C and 3.3 to 8.3 times at 125 °C in the SiC MOSFET compared to the Si IGBT with almost the same total power loss.

iii) The switching phenomenon of the MOSFET is almost independent of the operating temperature, while there is a strong temperature dependence in the Si IGBT. Simulation showed that at a switching frequency of 100 kHz and a junction temperature of 25 °C, the difference in efficiencies between the inverter with the SiC and the Si is 5.47 %, while this difference is 12.9 % at 125 °C. In particular, the reverse recovery current of the Si diode and the tail current of the IGBT worsens with increase in temperature.

Thus, the reduction in switching loss can be utilized in a number of ways to optimize the circuit design such as; increase efficiency, reduce cooling requirement. Most importantly, by increasing the operating frequency, the size of passive components can be reduced resulting in higher power density of the system.

References

[1] G. Spagnuolo et al., "Renewable Energy Operation and Conversion Schemes: A Summary of Discussions During the Seminar on Renewable Energy Systems," in IEEE Industrial Electronics Magazine, vol. 4, no. 1, pp. 38-51, March 2010.

[2] P. C. Zuk and B. Odekirk, "SiC Impacts Greening of Power - Understanding the Differences between Silicon Carbide (SiC) and Silicon (Si) for Power Electronics," in Power Systems Design Europe, ed, 2008, pp. 3436.

[3] B. Wrzecionko, J. Biela and J. W. Kolar, "SiC power semiconductors in HEVs: Influence of junction temperature on power density, chip utilization and efficiency," Industrial Electronics, 2009. IECON '09. 35th Annual Conference of IEEE, Porto, 2009, pp. 3834-3841.

[4] T. Evans, T. Hanada, Y. Nakano and T. Nakamura, "Development of SiC power devices and modules for automotive motor drive use," Future of Electron Devices, Kansai (IMFEDK), 2013 IEEE International Meeting for, Suita, 2013, pp. 116-117.

[5] G. Skibinski, D. Braun, D. Kirschnik and R. Lukaszewski, "Development in Hybrid Si-SiC Power Modules," ed: Rockewell Automation, 2006.

[6] Z. Zhang, F. Wang, L. M. Tolbert, B. J. Blalock and D. J. Costinett, "Evaluation of Switching Performance of SiC Devices in PWM Inverter-Fed Induction Motor Drives," in IEEE Transactions on Power Electronics, vol. 30, no. 10, pp. 5701-5711, Oct. 2015.

[7] T. Zhao, J. Wang, A. Q. Huang and A. Agarwal, "Comparisons of SiC MOSFET and Si IGBT Based Motor Drive Systems," Industry Applications Conference, 2007. 42nd IAS Annual Meeting. Conference Record of the 2007 IEEE, New Orleans, LA, 2007, pp. 331-335.

[8] J. Rice and J. Mookken, "Economics of High Efficiency SiC MOSFET based 3-ph Motor Drive," PCIM Europe 2014; International Exhibition and Conference for Power Electronics, Intelligent Motion, Renewable Energy and Energy Management; Proceedings of, Nuremberg, Germany, 2014, pp. 1-8.

[9] S. Tiwari, O. -M. Midtgård, T. M. Undeland and R. Lund, "Experimental performance comparison of six-pack SiC MOSFET and Si IGBT modules paralleled in a half-bridge configuration for high temperature applications," Wide Bandgap Power Devices and Applications (WiPDA), 2015 IEEE 3rd Workshop on, Blacksburg, VA, 2015, pp. 135-140.

[10] S. Tiwari, I. Abuishmais, T. Undeland and K. Boysen, "Silicon carbide power transistors for photovoltaic applications," PowerTech, 2011 IEEE Trondheim, Trondheim, 2011, pp. 1-6.

[11] S. Tiwari et al., "Design considerations and laboratory testing of power circuits for parallel operation of silicon carbide MOSFETs," Power Electronics and Applications (EPE'15 ECCE-Europe), 2015 17th European Conference on, Geneva, 2015, pp. 1-10.

[12] A. Agarwal, R. Singh, S. -H. Ryu, J. Richmond, C. Capell, S. Schwab, et al., "600 V, 1- 40 A, Schottky Diodes in SiC and Their Applications."

[13] D. Heer and A. K. Bayoumi, "Switching characteristics of modern 6.5kV IGBT/Diode," PCIM Europe 2014; International Exhibition and Conference for Power Electronics, Intelligent Motion, Renewable Energy and Energy Management; Proceedings of, Nuremberg, Germany, 2014, pp. 1-8.

[14] "SiC MOSFET Isolated Gate Driver," App. Note, CPWR-AN10 Rev. C, Cree, Inc., Durham, NC 27703, 2014.

[15] "CCS050M12CM2 Datasheet," Cree, Inc., 2014.

[16] "FS75R12KT4_B15 Datasheet Rev. 3," Infineon, Inc., 2013.